

# LOW $Q^2$ STRUCTURE FUNCTION MEASUREMENTS

Gregorio Bernardi  
 H1 Collaboration

LPNHE-Paris, 4 place Jussieu, 75252 Paris Cedex 05, France

## Abstract

New results <sup>1</sup> on the measurement of the proton structure function  $F_2(x, Q^2)$  are reported for momentum transfers squared  $Q^2 \geq 1.5 \text{ GeV}^2$  and Bjorken  $x \geq 3.5 \cdot 10^{-5}$ , using data collected by the HERA experiments H1 and ZEUS in 1994.  $F_2$  increases significantly with decreasing  $x$ , even in the lowest reachable  $Q^2$  region. The data are well described by a Next to Leading Order QCD fit, and support within the present precision that the rise at low  $x$  within this  $Q^2$  range is generated via the DGLAP evolution equations. A comparison with models based on pomeron exchange is also presented. The gluon density is extracted and observed to rise at low  $x$ .

## 1 Introduction

The HERA  $ep$  collider has been designed to study Deep Inelastic Scattering (DIS) at very high  $Q^2$  where substructure of quarks could be observed. However in the first 3 years of data operation, which allowed a steady growth towards the design luminosity of the machine, most of the interest has focused on the study of low  $x$ , low  $Q^2$  DIS, where new tests of perturbative QCD can be performed. The first observations on the 1992 data showed a rise of the proton structure function  $F_2(x, Q^2)$  at low  $x < 10^{-2}$  with decreasing  $x$  [3, 4], which was confirmed with the more precise data of 1993 [5, 6]. Such a behaviour is qualitatively expected in the double leading log limit of Quantum Chromodynamics [7]. It is, however, not clarified whether the linear QCD evolution equations, as the conventional DGLAP evolution [8] in  $\ln Q^2$  and/or the BFKL evolution [9] in  $\ln(1/x)$ , describe the rise of  $F_2$  or whether there is a significant effect due to nonlinear parton recombination [10]. At low  $Q^2$  ( $\leq 5 \text{ GeV}^2$ ) the new results can be confronted to Regge inspired models, which expects a rather flat behaviour as a function of  $x$ , in order to study the transition between DIS and photoproduction. The 1994 data have allowed to reach  $Q^2=1.5 \text{ GeV}^2$  and confirm the persistence of the rise at low  $x$ . The measurements have been achieved by using dedicated data samples (sect. 2) and are discussed and analyzed in terms of perturbative QCD in sect. 3.

## 2 Structure Function Measurement

In 1994 both experiments have reduced the minimum  $Q^2$  at which they could measure  $F_2$  using several techniques: i) both experiments were able to diminish the region around the backward beam pipe in which the electron could not be measured reliably in 93, thus increasing the maximum polar angle of the scattered electron (measured w.r.t. to proton beam direction). This large statistic

---

<sup>1</sup>Talk given at the 2<sup>nd</sup> Rencontres du Vietnam, held in Hô Chi Min City in October 1995. The results presented here are extracted from the recent publications of the the H1 and ZEUS collaborations [1, 2].

sample, taken with the nominal HERA conditions has an integrated luminosity of about  $3 \text{ pb}^{-1}$ . ii) An integrated luminosity of  $\sim 60 \text{ nb}^{-1}$  of data was collected for which the interaction point was shifted by  $+62 \text{ cm}$ , in the forward direction, resulting in an increase of the electron acceptance (so-called "shifted vertex" data sample). iii) Both experiments used DIS events which underwent initial state photon radiation detected in an appropriate photon tagger to measure  $F_2$  at lower  $Q^2$  (so called "radiative" sample). The incident electron energy which participate in the hard scattering is thus reduced, and so is the  $Q^2$ . The luminosity was determined from the measured cross section of the Bethe-Heitler reaction  $e^-p \rightarrow e^-p\gamma$ , measuring the hard photon bremsstrahlung data only. The precision of the luminosity measurement is 1.5% (3.9% for the shifted vertex data).

The kinematic variables of the inclusive scattering process  $ep \rightarrow eX$  can be reconstructed in different ways using measured quantities from the hadronic final state and from the scattered electron. The choice of the reconstruction method for  $Q^2$  and  $y$  determines the size of systematic errors, acceptance and radiative corrections. The measurements presented here have been obtained with the electron (E) and with the  $\Sigma$  methods [11] for which the  $y$ ,  $Q^2$  and  $x$  formulae are

$$y_e = 1 - \frac{E'_e}{E_e} \sin^2 \frac{\theta_e}{2} \quad y_\Sigma = \frac{\Sigma}{\Sigma + E'_e(1 - \cos \theta_e)} \quad Q_{e,\Sigma}^2 = \frac{E_e'^2 \sin^2 \theta_e}{1 - y_{e,\Sigma}} \quad x_{e,\Sigma} = \frac{Q_{e,\Sigma}^2}{s y_{e,\Sigma}} \quad (1)$$

and  $E, p_x, p_y, p_z$  are the four-momentum vector components of each particle,  $E_e$  is the electron beam energy,  $s$  the squared center of mass energy of the collision,  $\Sigma \equiv \sum_h E_h - p_{z,h}$  and the summation is done over all hadronic final state particles neglecting their masses. The E method, which is independent of the hadronic final state, apart from the requirement that the interaction vertex is reconstructed using the final state hadrons, has at large  $y$  the best resolution in  $x$  and  $Q^2$  but needs sizeable radiative corrections. At low  $y$  the E method is not applied due to the degradation of the  $y_e$  resolution as  $1/y$ . The  $\Sigma$  method, which has small radiative corrections, relies mostly on the hadronic measurement which has still an acceptable resolution at low  $y$  values and can be used from very low to large  $y$  values. H1 measures  $F_2$  with the E and the  $\Sigma$  method and after a complete consistency check, in particular at low  $x$ , uses the E method for  $y > 0.15$  and the  $\Sigma$  method for  $y < 0.15$ . ZEUS measures  $F_2$  at low  $Q^2$  with the E method.

The event selection is similar in the two experiments. Events are filtered on-line using calorimetric triggers which request an electromagnetic cluster of at least 5 GeV not vetoed by a trigger element signing a beam background event. Offline, further electron identification criteria are applied (track-cluster link, shower shape and radius) and a minimum energy of 8(11) GeV is requested in ZEUS(H1). H1 requests a reconstructed vertex within  $3\sigma$  of the expected interaction position, while ZEUS requires that the quantity  $\delta = \Sigma + E'_e(1 - \cos \theta)$  satisfies  $35 \text{ GeV} < \delta < 65 \text{ GeV}$ . If no particle escapes detection,  $\delta = 2E = 55 \text{ GeV}$ , so the  $\delta$  cut reduces the photoproduction background and the size of the radiative corrections. The only significant background left after the selection comes from photoproduction in which a hadronic shower or a photon fakes an electron. In H1 for instance, it has been estimated consistently both from the data and from Monte Carlo simulation and amounts to less than 3% except in a few bins where it can reach values up to 15%. It is subtracted statistically bin by bin and an error of 30% is assigned to it.

The acceptance and the response of the detector has been studied and understood in great detail by the two experiments: more than two millions Monte Carlo DIS events were generated using DJANGO [12] and different quark distribution parametrizations, corresponding to an integrated luminosity of approximately  $20 \text{ pb}^{-1}$ . The program is based on HERACLES [13] for the electroweak interaction and on LEPTO [14] and ARIADNE [15] to simulate the hadronic final state. HERACLES includes first order radiative corrections, the simulation of real bremsstrahlung photons and the longitudinal structure function. For the parton densities, the GRV [16] and the MRS parametrizations [17] were used. The Monte Carlo events, after a detailed simulation based on the GEANT program, were subject to the same reconstruction and analysis chain as the real data.

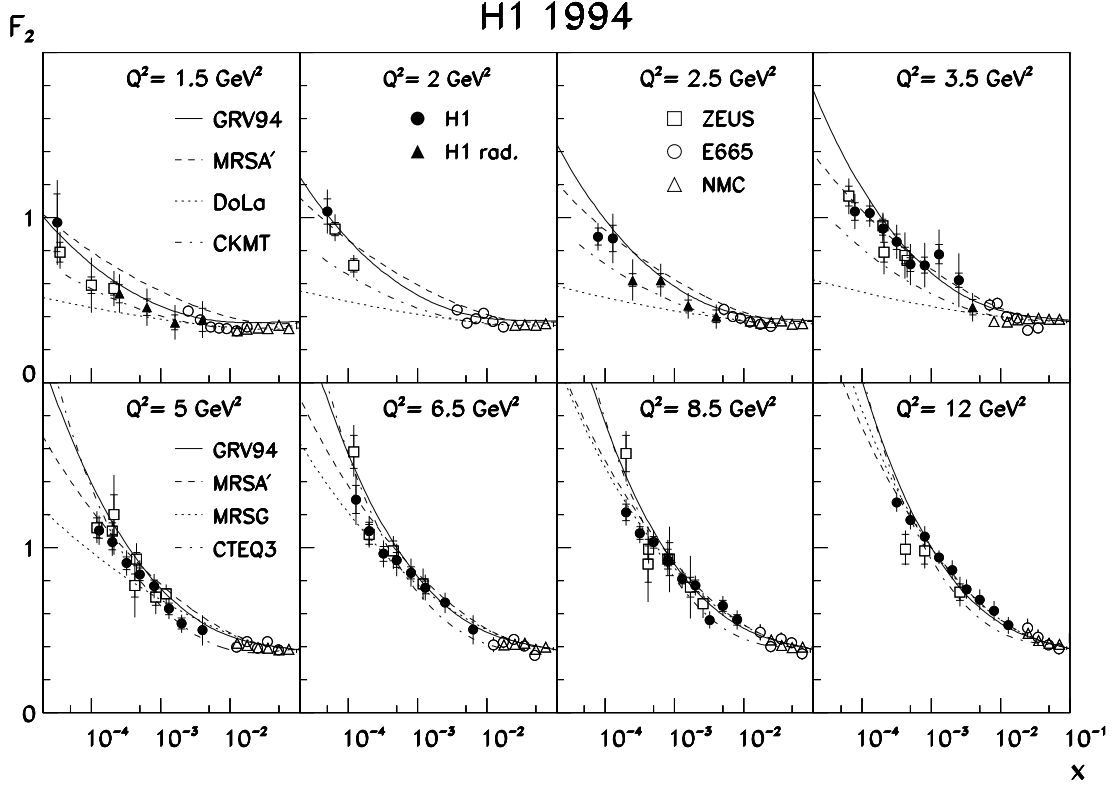


Figure 1: Measurements of the proton structure function  $F_2(x, Q^2)$  in the low  $Q^2$  region by H1 and ZEUS are shown together with the results from the E665 and NMC fixed target experiments. Different  $F_2$  parametrizations are confronted to the data: DOLA and CKMT (only in the upper row of  $Q^2$  bins); CTEQ3M, MRSG and MRSA' (lower row); GRV is shown for the full range.

The structure function  $F_2(x, Q^2)$  was derived after radiative corrections from the one-photon exchange cross section since effects due to  $Z$  boson exchange are smaller than 1% at low  $Q^2$ .

$$\frac{d^2\sigma}{dx dQ^2} = \frac{2\pi\alpha^2}{Q^4 x} \left(2 - 2y + \frac{y^2}{1+R}\right) F_2(x, Q^2) \quad (2)$$

The ratio  $R = F_2/2xF_1 - 1$  was calculated using the QCD relation [18]. With the different data sets available detailed cross checks could be made in the kinematic regions of overlap. The results were found to be in very good agreement with each other for all kinematic reconstruction methods used, and the effect of systematic errors could be monitored: for the E method the main source of error are the energy calibration (known at the 1% level), the knowledge of the electron identification efficiency, the error on the polar angle of the scattered electron, ( $\delta\theta = 1\text{mrad}$ ) and the radiative corrections at low  $x$ . For the  $\Sigma$  method, the knowledge of the absolute energy scale for the hadrons, the fraction of hadrons which stay undetected in particular at low  $x$ , due to calorimetric thresholds and to a lesser extent the electron energy calibration are the dominating factors. Further uncertainties common to all methods (selection, structure function dependence etc.) were also taken into account. The total  $F_2$  errors on the 1994 data ranges between 5 to 10% in the 10-100  $\text{GeV}^2$  range and between 10 to 20% below 10  $\text{GeV}^2$ . The final results on the 1994 data of H1 and ZEUS are shown in fig. 1 in the new kinematic domain reached using the radiative and the shifted vertex data. Compared to the 1993 data analyses the  $F_2$  measurement has been extended to lower  $x$  (from  $1.8 \cdot 10^{-4}$  to  $3.5 \cdot 10^{-5}$ ) and  $Q^2$  (from  $4.5 \text{ GeV}^2$  to  $1.5 \text{ GeV}^2$ ). Both experiments are in good agreement and show that the  $F_2$  rise at low  $x$  persist, albeit less strongly,

down to the lowest measured  $Q^2=1.5 \text{ GeV}^2$ . A smooth transition to the fixed target experiments E665 [19] and NMC [20] is observed with the low  $y$  results of H1, allowing to confront all these results to theoretical expectations.

### 3 Low $Q^2$ and Perturbative QCD

In fig. 1 are also shown the extrapolations of the  $F_2$  parametrizations based on some theoretical model fitted to the previous data. They can be divided in two categories: one, motivated by Regge theory, assumes a pomeron exchange as a dynamical basis and successfully describes the behaviour of the total cross-sections of photoproduction and hadron-hadron collisions; the other is based on perturbative QCD and is known to well describe the DIS regime, but is expected to break down for a given  $x$  at some low  $Q^2$ . The Regge models were expected to work at least at low  $Q^2$ , but the DOLA parametrization which uses a “soft” pomeron (intercept  $\simeq 1.08$ ) [22] largely underestimate  $F_2$  at low  $x$  even at  $1.5 \text{ GeV}^2$ . The CKMT model [23], which assumes that in the present  $Q^2$  range the “bare” pomeron becomes visible and has a higher trajectory intercept ( $\simeq 1.24$ ), predicts a weaker rise at low  $x$  than observed, except maybe at  $1.5 \text{ GeV}^2$ . These comparisons underline the difference between the behaviour of the total cross-section of real and virtual photons, since in the HERA kinematic domain and using the Hand [24] definition of the photon flux  $\sigma_{tot}^{\gamma^*P}$  can be expressed as  $\sigma_{tot}^{\gamma^*P}(x, Q^2) \simeq \frac{4\pi^2\alpha}{Q^2} F_2(x, Q^2)$ .

The parametrizations based on the DGLAP QCD evolution equations describe the data remarkably well, as expected above  $5\text{-}10 \text{ GeV}^2$ , but surprizingly at values around 1 or  $2 \text{ GeV}^2$  where non-perturbative effects were believed to distort the DGLAP picture. The MRSA’ parametrizations of the parton densities are defined at  $Q_0^2 = 4 \text{ GeV}^2$ , then evolved in  $Q^2$  and fitted to previous experimental data, including the 1993 HERA data. The agreement observed above  $10 \text{ GeV}^2$  confirms that the 1993 and 1994 HERA results are compatible. Between  $1.5$  and  $10 \text{ GeV}^2$  the good description tells us that within the present precision perturbative QCD can be applied in this range. More striking is the confirmation of the pre-HERA prediction of the  $F_2$  rise at low  $x$  by the

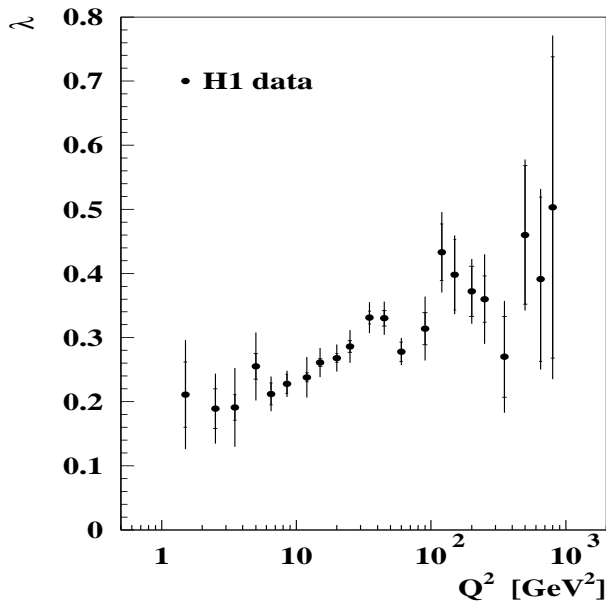


Figure 2: Variation of the exponent  $\lambda$  from fits of the form  $F_2 \sim x^{-\lambda}$  at fixed  $Q^2$  values.

GRV model [25] which conjectured at a very low energy scale ( $\mu^2=0.34 \text{ GeV}^2$ ) that the proton is formed by valence-like partons as shown in fig. 4 and that the DGLAP equations can be applied to generate “radiatively” the rise of the gluon and sea-quark density at low  $x$ , when evolving towards higher  $Q^2$ . The H1 and ZEUS results are very well described by the GRV model at low  $Q^2$  as can be seen in fig. 1 but also in the full HERA kinematic range, from 1.5 to 5000  $\text{GeV}^2$  [26]. This success support the idea that the rise at low  $x$  is a direct consequence of the DGLAP equations, and that non-perturbative effects are relatively weak at low  $x$  and low  $Q^2$ . The evolution with  $Q^2$  of the strength of the rise can be quantified by fitting an  $x^{-\lambda}$  (or equivalently a  $W^{2\lambda}$ ,  $W$  being the invariant mass of the  $\gamma^* - p$  system) function at fixed  $Q^2$  to  $F_2(x), x < 0.1$ . The values of  $\lambda$  obtained by the fit in each  $Q^2$  bin are displayed in fig 2 and clearly confirm the long time prediction made for asymptotic free field theories like QCD [7] of a rise of  $F_2$  at low  $x$ , and that the strength of this rise increases with  $Q^2$ . With the present data, it is however not possible to know precisely this strength below 5  $\text{GeV}^2$ , thereby postponing a definite test of perturbative QCD in this region.

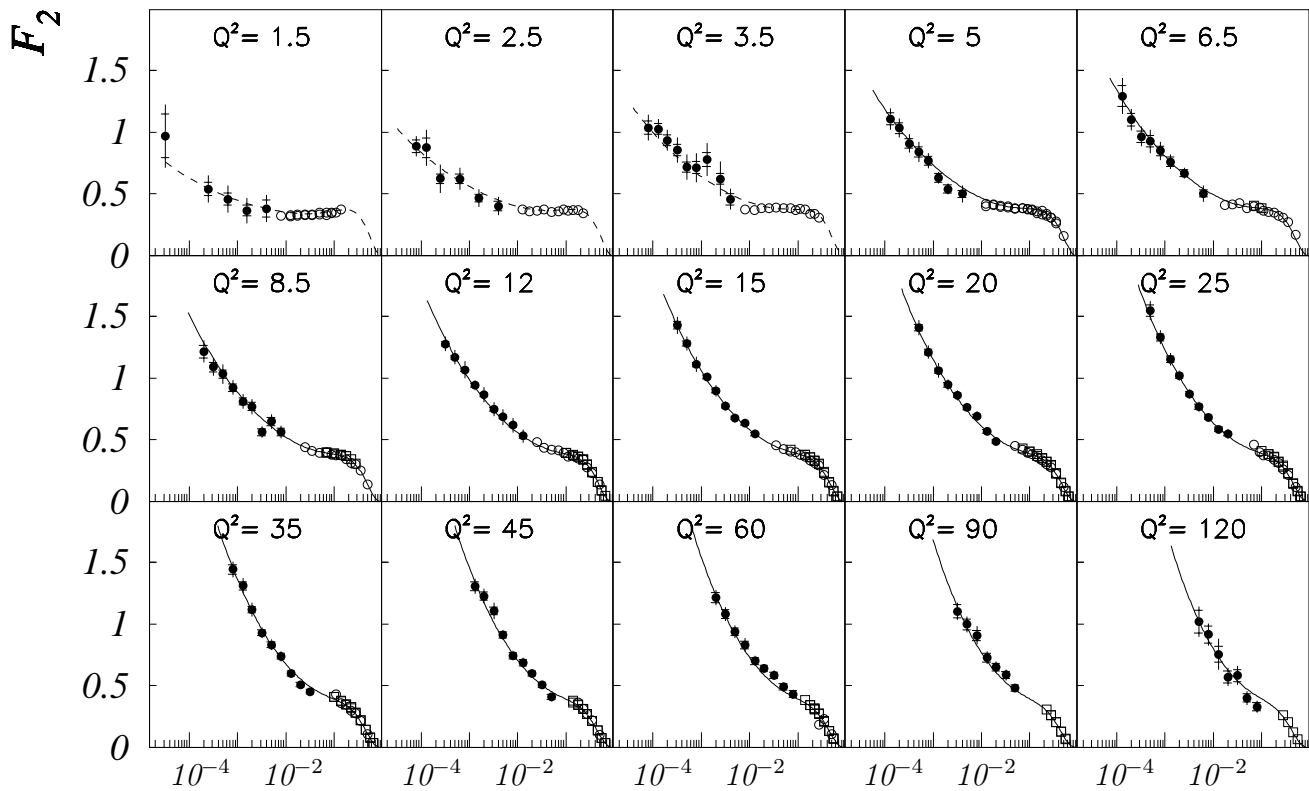


Figure 3: H1 measurement (black circles) of the proton structure function  $F_2(x, Q^2)$  as function of  $x$  in different bins of  $Q^2$ . The inner error bar is the statistical error. The full error represents the statistical and systematic errors added in quadrature. The curve represent a NLO QCD fit to the H1, BCDMS (open squares) and NMC (open circles) data at  $Q^2 > 5 \text{ GeV}^2$ .

To make fully use of the new precision reached with the 1994 data, the H1 collaboration has performed a Next-to-Leading Order (NLO) QCD fit on the H1, BCDMS and NMC data with the conditions  $Q^2 > 5 \text{ GeV}^2$ , and  $x < 0.5$  if  $Q^2 < 15 \text{ GeV}^2$  to avoid higher-twists effects. The H1 measurements which extend up to 5000  $\text{GeV}^2$  (they are shown up to 120  $\text{GeV}^2$  in fig. 3) were fitted successfully and allow to constrain the gluon density at low  $x$ . The parton densities were parametrized at  $Q_0^2=5 \text{ GeV}^2$ , in particular the gluon was expressed with 3 parameters as  $xg(x) = A_g x^{B_g} (1-x)^{C_g}$ . The quark and antiquark components of the sea were assumed to be equal, and  $\bar{u}$  set equal to  $\bar{d}$ . As determined in [27], the strange quark density was taken to be  $\bar{s} = (\bar{u} + \bar{d})/4$ . Further constraints were coming from the quark counting rules and the momentum

sum rules. For  $\Lambda$  the value of 263 MeV was taken [29]. A detailed treatment of the  $F_2$  errors propagation on the gluon density has been done, resulting in the error bands of fig 4b which represent  $xg(x)$  at 5 and 20 GeV<sup>2</sup>. A variation of  $\Lambda$  by 65 MeV gives a change of 9% on the gluon density at 20 GeV<sup>2</sup> which has not been added to the error bands. The accuracy of this determination of  $xg$  is better by about a factor of two than the H1 result based on the 1993 data [28].

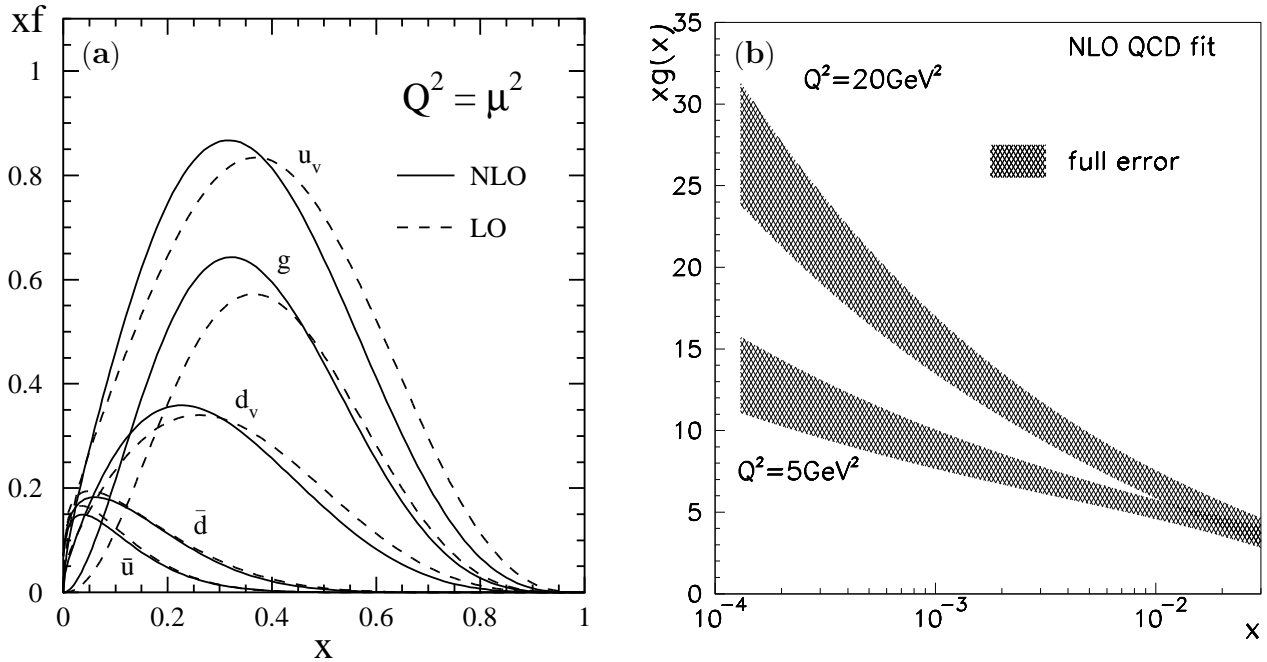


Figure 4: a) Parton densities (valence quarks ( $u_v, d_v$ ), gluon ( $g$ ) and sea quarks) of the GRV model at the initial energy scale  $\mu^2 = 0.34 \text{ GeV}^2$ . b) Gluon density at 5 and 20 GeV<sup>2</sup> determined by a NLO fit to the H1, NMC and BCDMS data. The error bands represent the full error except for the uncertainty on  $\Lambda$ .

A rise of the gluon density towards low  $x$  is observed which is related to the behaviour of  $F_2 \propto x^{-\lambda}$ . Accordingly, the rise of  $xg$  towards low  $x$  increases with increasing  $Q^2$ . Finally we can observe in fig. 3 that the data at  $Q^2 < 5 \text{ GeV}^2$ , which were excluded from the fit, are still well reproduced by the fit evolved backwards in  $Q^2$ . More data at low  $x$  and  $Q^2 < 1 \text{ GeV}^2$  are nevertheless needed to be able to test the hypothesis of a gluon density which would take the valence-like shape displayed in fig. 4a when  $Q^2 \rightarrow 0.3 \text{ GeV}^2$ , and more generally, to better understand the dynamics at low  $Q^2$  and high parton densities. The HERA experiments, which have last year upgraded the capabilities of their backward detectors, will be able to reach these low  $Q^2$  with the data taken in 1995 and 1996.

## Acknowledgements

I would like to thank the organizers and in particular Kim and J. Trần Thanh Vân to have realized such an interesting and fruitful exchange workshop in this fascinating country. I would also like to thank my close collaborators, Ursula Bassler, Beatriz Gonzalez-Pineiro and Fabian Zomer, all the friends of the H1 structure function group and the H1 and ZEUS collaboration with whom we obtained the results described above. Special thanks also to Marie for her constant help and support, and for sharing our unforgettable vietnamese journey.

## References

- [1] ZEUS Collab., M. Derrick et al., DESY 95-193 (1995), Subm. to Phys. Lett.
- [2] H1 Collab., I. Abt et al., DESY 96-039 (1996), Subm. to Nucl. Phys.
- [3] H1 Collab., I. Abt et al., Nucl. Phys. **B407** (1993) 515.
- [4] ZEUS Collab., M. Derrick et al., Phys. Lett. **B316** (1993) 412.
- [5] H1 Collab., T. Ahmed et al., Nucl. Phys. **B439** (1995) 471.
- [6] ZEUS Collab., M. Derrick et al., Z. Phys. **C65** (1995), 379.
- [7] A. De Rújula et al, Phys. Rev. **D10** (1974) 1649.
- [8] Yu. L. Dokshitzer, Sov. Phys. JETP **46** (1977) 641;  
V. N. Gribov and L.N. Lipatov, Sov. J. Nucl. Phys. **15** (1972) 438 and 675;  
G. Altarelli and G. Parisi, Nucl. Phys. **B126** (1977) 297.
- [9] E. A. Kuraev, L. N. Lipatov and V. S. Fadin, Sov. Phys. JETP **45** (1977) 19; 9;  
Y. Y. Balitsky and L.N. Lipatov, Sov. J. Nucl. Phys. **28** (1978) 822.
- [10] L. V. Gribov, E. M. Levin and M. G. Ryskin, Phys. Rep. **100** (1983) 1;  
A. H. Mueller and N. Quiu, Nucl. Phys. **B268** (1986) 427.
- [11] U. Bassler and G. Bernardi, Nucl. Instr. and Meth. **A361** (1995) 197.
- [12] G. A. Schuler and H. Spiesberger, Proceedings of the Workshop Physics at HERA, vol. 3, eds. W. Buchmüller, G. Ingelman, DESY (1992) 1419.
- [13] A. Kwiatkowski, H. Spiesberger and H.-J. Möhring, Computer Phys. Comm. **69** (1992) 155.
- [14] G. Ingelman, Proceedings of the Workshop Physics at HERA, vol. 3, eds. W. Buchmüller, G. Ingelman, DESY (1992) 1366.
- [15] L. Lönnblad, Computer Phys. Comm. **71** (1992) 15.
- [16] M. Gluck, E. Reya and A. Vogt, Z. Phys. **C67** (1995) 433.
- [17] A.D. Martin, W.J. Stirling and R.G. Roberts, RAL preprint RAL-95-021 (1995).
- [18] G. Altarelli and G. Martinelli, Phys. Lett. **B76** (1978) 89.
- [19] E665 Collab., M.R. Adams et al., Phys. Rev. Lett. **75** (1995) 1466.
- [20] NMC Collab., P. Amaudruz et al., Phys. Lett. **B259** (1992) 159.
- [21] BCDMS Collab., A. C. Benvenuti et al., Phys. Lett. **B237** (1990) 592.
- [22] A. Donnachie and P. V. Landshoff, Z. Phys. **C61** (1994) 139.
- [23] A. Capella et al., Phys. Lett. **B337** (1994) 358.
- [24] L.N. Hand, Phys. Rev. **129** (1963) 1834.
- [25] M. Glück, E. Hoffmann and E. Reya, Z. Phys. **C13** (1982) 119.
- [26] G. Bernardi, LPNHE-preprint 96-01 (1996), hep-ex/9603008, to appear in the Proceedings of the XXVI<sup>th</sup> Workshop on High Energy Physics, Gravitation and Field Theory, Protvino (Russia).
- [27] CCFR Collaboration, A.O. Bazarko et al., Z. Phys. **C65** (1995) 189.
- [28] H1 Collaboration, S. Aid et al., Phys. Lett. **B354** (1995) 494.
- [29] M. Virchaux and A. Milsztajn, Phys. Lett. **B274** (1992) 221.
- [30] H1 Collab., S. Aid et al., Phys. Lett. **B354** 494 (1995).